Relaxation Kinetics of Micellization in Micelle-Forming Block Copolymer in Selective Solvent

Chikako Honda* and Yukiyo Abe

Showa College of Pharmaceutical Sciences, Higashitamagawagakuen 3-3165, Machida-shi, Tokyo 194, Japan

Takuhei Nose

Department of Polymer Chemistry, Tokyo Institute of Technology, Ookayama, Meguro-ku, Tokyo 152, Japan

Received May 20, 1996[⊗]

ABSTRACT: Relaxation kinetics of micelle-forming poly(α-methylstyrene)-*block*-poly(vinylphenethyl alcohol) (PαMS-*b*-PVPA) in a selective solvent, benzyl alcohol (BA), has been investigated by time-resolved static light scattering. The time evolution of apparent molecular weight (M_{wapp}) and radius of gyration (R_{gapp}) were measured in the course of micellar relaxation, which was induced by temperature jumps (T-jumps) within the micellar region. The following two types of T-jumps were performed: (1) type I, a T-jump from shallow T-depth to deep T-depth with the change in depth, ΔT, being defined by $\Delta T = \text{cmt} - T$ (cmt, the critical micelle temperature), and (2) type II, a T-jump from deep ΔT_0 to shallow ΔT with $\Delta T_0 > \Delta T$. In a type I T-jump, the majority of existing unimers form new micelles and some of unimers enter into existing micelles formed in the premicellization. In a type II T-jump, instead of monotonical changes in micellar fraction and size from the starting state to the final state, the micelles first decompose with dominantly decreasing micellar size, and then the micellar size recovers to approach the final size. The change of M_{wapp} in the type I T-jump is characterized by a time constant (τ_I) which decreases with increasing the polymer concentration. The τ_I is almost equal to the time constant of the fast process in the direct micellization from unimer state (τ_1). The relaxation processes in the type II T-jump are described by time constants τ_D and τ_R for micelle decomposition and recovery, respectively. τ_D is much smaller than τ_R, having no concentration dependence, while τ_R has a concentration dependence, having almost the same value as τ_1. The occurrence of micellar decomposition as the first process in the type II T-jump is thermodynamically interpreted by a phenomenological theory.

Introduction

Micelle formation of block copolymers in selective solvent has extensively been studied theoretically and experimentally.[2,16−29] However, a few studies on the micellization kinetics have been reported for polymeric systems.[16,17,21−27] Considerable efforts have been devoted to studies of relaxation kinetics for surface active agents of low molecular weight substances.[1,3−15] The association or dissociation from one equilibrium to another equilibrium state takes place essentially by two processes.[5] The faster process is associated with the redistribution of association number of each micelle with no change of the total number of micelles, while the slower process is to approach the final equilibrium by simultaneous proceedings of micelle formation and decomposition with changing the total number of micelles. This idea was theoretically described for the first time by Aniansson and Wall (A−W).[3] A basic assumption in the A−W theory is that all the changes proceed by an elementary process of expulsion/entry of a unimer from/into the micelle. This interpretation has been confirmed by many experiments using chemical−relaxation techniques[1,4,6−9,11,12,14] and theoretically discussed to a large extent.[5,10,13,22]

For block copolymers, the relaxation time for a polymer chain escaping from the micelle has theoretically been discussed on the basis of scaling analysis.[18−20] Fission and fusion of polymer micelles have been considered to be less likely than expulsion and entry of the unimer.[18,19] Tuzar and co-workers[16] observed micelle formation and decomposition of block copolymers by a stopped-flow method with light scattering and found that the relaxation time of micellar formation was on the order of 10 ms, while the decomposition occurred much faster. Recent experiments[17,27] on micellization process support the above considerations on the basis of the mechanism of unimer expulsion and entry. On the other hand, Mattice et al.[21−26] have performed computer simulation and fluorescence experiments for micellization of block copolymers that suggest the presence of two processes with different time scales and the possibility of involving another mechanism such as the fission and fusion.

In our previous paper,[27] by means of time-resolved light scattering, we studied the micellization process in the course of micellization after quenching from the unimer region to the micelle region using poly(α-methylstyrene)-*block*-poly(vinylphenethyl alcohol) in benzyl alcohol. The process was so slow that it could be observed by light-scattering measurements. It has been demonstrated that the micellization proceeds stepwise in two processes with different rates, similar to those of low molecular weight surfactants.

In this study, for better understanding of these micellization processes, we investigate the relaxation process with changing temperature from one equilibrium state to another, that is, the micellar kinetic processes of changes in micellar size and micellar-forming fraction induced by temperature jumps within the micellar region. We may more clearly see the two essential processes in micellar relaxation by the temperature jump within the micellar region. In fact, we have successfully observed the two processes of decomposition and recovery of micelles, which have never been observed so clearly before, to our knowledge.

We have selected the system poly(α-methylstyrene)-*block*-poly(vinylphenethyl alcohol) in benzyl alcohol near

[⊗] Abstract published in *Advance ACS Abstracts,* September 15, 1996.

S0024-9297(96)00735-8 CCC: $12.00

Table 1. Molecular Weight and Composition of Block Copolymer

sample code	$M_{P\alpha MS} \times 10^{-4}$	$M_{PVPA} \times 10^{-4}$	$M_{total} \times 10^{-4}$	ϕ_{PVPA}[a]
KT-327	11.3	1.23	12.5	0.08

[a] ϕ_{PVPA}: PVPA composition in fractional degrees of polymerization.

the critical micellization temperature and used time-resolved light scattering to observe the processes, similar to the previous study. Apparent molecular weight (M_{wapp}) and radius of gyration (R_{gapp}) obtained by light scattering give differently weighted averages of association number and size of the associated particle in solution, respectively, which enables us to tell which process dominates over the other in the relaxation, the size growth or the association-number increase.[27,31]

In the following sections, we will first describe the present solution system, light-scattering measurements, and conditions of temperature jumps. Then, the experimental results will be presented and analyzed to evaluate time constants for the relaxation processes. Thermodynamic interpretation will also be given for the time evolution of M_{wapp} and R_{gapp}.

Experimental Section

Materials. Poly(α-methylstyrene)-*block*-poly(*p*-vinylphenethyl alcohol) (PαMS-*b*-PVPA) with a sample code KT-327 was anionically polymerized,[30] and its characteristics are listed in Table 1. The molecular weight distribution index (M_w/M_n) was around 1.1. The benzyl alcohol (BA) purchased was used without further purification. BA is a good solvent of PVPA and a nonsolvent of PαMS, so that the PαMS block may segregate to form a core and the PVPA block may make a corona when the copolymer forms a micelle. In fact, it was found in our previous work[31] that KT-327 formed crew-cut star-shaped micelles in *m*-chlorobenzyl alcohol.

Light-Scattering Measurements. Static light-scattering measurements were carried out in the same way as in the previous study.[28] The light-scattering apparatus was a DLS-700 of Ohtsuka Electronic Co. Ltd., with an Ar ion laser operated at 488 nm as light source. Optically purified homogeneous sample solutions were prepared, with the concentration ranging from 2×10^{-4} to 8×10^{-4} g(g of solution)$^{-1}$.

Integrated intensity of scattered light was measured as a function of scattering angle, θ, where it took about 3 min to measure a set of data, which was much shorter than the experimental time scale of micellar relaxation, so that no correction of time lag was made. Excess Rayleigh ratio $\Delta R(\theta)$ was calculated from the measured excess scattered intensity using the intensity of benzene as standard. Since the present time-resolved measurements do not enable to use the conventional analysis with the extrapolation to the dilute limit, we evaluated apparent molecular weight (M_{wapp}) and apparent radius of gyration (R_{gapp}) without the extrapolation, which are defined as

$$M_{wapp} = \frac{\Delta R(0)}{Kc} \tag{1}$$

$$R_{gapp}{}^2 = \frac{3\lambda_0{}^2 M_{wapp}(\text{initial slope})}{16\pi^2 n^2} \tag{2}$$

where c is the polymer concentration in grams per milliliter and K is the optical constant defined by $K = 4\pi^2 n^2 (dn/dc)^2/\lambda^4 N_A$, with n, λ_0, and N_A being the refractive index, the wavelength of incident beam, and the Avogadro constant, respectively. $Kc/\Delta R(0)$ and (initial slope) are the intercept and the initial slope of the Zimm plot, $Kc/\Delta R(\theta)$ vs $\sin^2(\theta/2)$, at finite concentrations. The refractive index increment (dn/dc) for the present solution was 0.0671 mL g^{-1}.[27] Because of the small content and small (dn/dc) value of PVPA, the obtained R_{gapp} can be regarded as the $\langle R_g{}^2 \rangle$ of the PαMS part of the block copolymer (micelle).

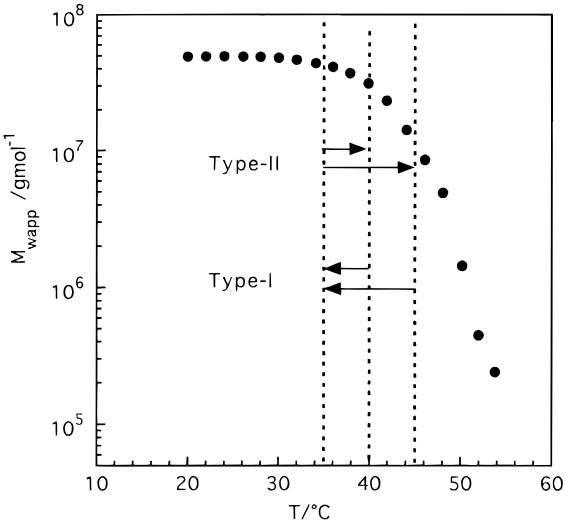

Figure 1. Change of M_{wapp} with decreasing temperature (T) for KT-327 (●) and conditions of the temperature jumps.

KT-327 started to form micelles around 50 °C with cooling at the rate of 2 °C/30 min, as shown in Figure 1. First, micelles were completely decomposed at 60 °C, and then, the micellization was performed at 35, 40, and 45 °C for about 200 h. After the premicellization, the micelle-forming solutions were quenched or heated to desired temperature, T, to observe the relaxation processes (Figure 1). Defining the temperature depth from the critical micelle temperature, cmt, as $T = \text{cmt} - T$, T-jumps from the premicellization temperature T_0 to the temperature T can be classified into two types: type I, the T-jump with $\Delta T_0 < \Delta T$ (shallow-to-deep jump), and type II, the T-jump with $\Delta T_0 > \Delta T$ (deep-to-shallow jump).

Results and Discussion

Premicellizations. The M_{wapp} and R_{gapp} of solutions after the premicellization at three temperatures, 35, 40, and 45 °C, are shown as a function of concentration in Figure 2. At the deepest quench, 35 °C, both M_{wapp} and R_{gapp} are almost independent of the concentration. This implies that most of polymers formed micelles at any concentrations in the present concentration range; in other words, the critical micelle concentration, cmc, at 35 °C is much lower than the experimental concentrations. On the other hand, at shallower quenches, 40 and 45 °C, M_{wapp} decreases with decreasing concentration, while R_{gapp} remains constant. This indicates that micellar fraction, which gives most of scattered light intensity, decreases with decreasing concentration and that the cmc is not much lower than the experimental range of concentration. The micellar fraction (θ_m) in the total polymer is approximately given by the ratio of $(M_{wapp} - M_{wunim})/(M_{wmic} - M_{wunim})$, where the M_{wmic} and M_{wunim} are molecular weights of micelles and unimers, respectively.[28,32] M_{wmic} can be estimated from the value of R_{gapp} with the relation R_g and M_w for micelles.[27,31] Namely, the relation $R_{gapp}/\text{nm} = 0.147 M_{wmic}{}^{0.3}$ is here used, on the basis of the approximation $R_g = R_{gapp}$, which is available for a large association number, where the exponent 0.3 is based on a spherical micelle,[27,31] and the prefactor 0.147 is determined such that the micellar fraction (θ_m) is unity for micellar solutions of higher concentrations at 35 °C. Estimated θ_m values are shown in Figure 2. The micellar fraction decreases with decreasing concentration at 40 and 45 °C, and the cmc corresponds to a concentration at which the micellar fraction vanishes. At the shallowest quench, 45 °C, an

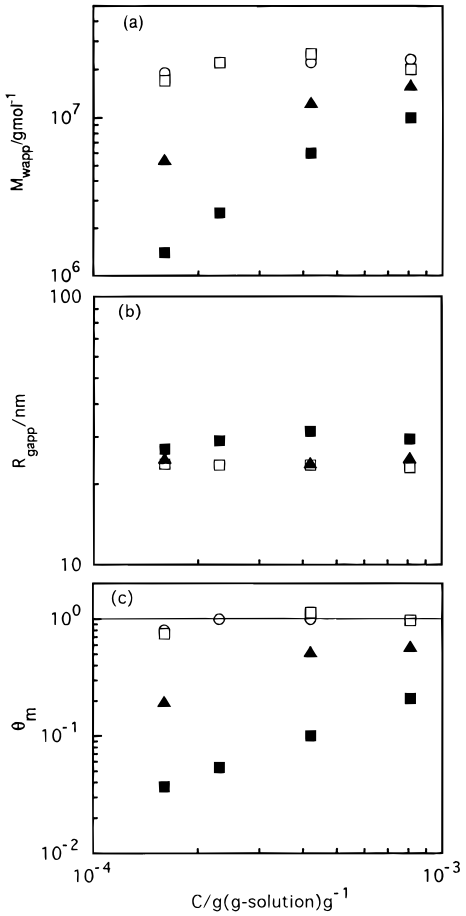

Figure 2. M_{wapp}, R_{gapp}, and estimated micellar fractions (θ_m) in solution at the end of the premicellizations at 35 °C (○, □), 40 °C (▲), and 45 °C (■) as a function of concentration.

appreciable fraction of polymers remain as unimers, in particular, at lower concentrations.

Relaxation of Micellization in Type I T-Jumps (Shallow-to-Deep Jumps). In Figures 3 and 4 are shown log−log plots of M_{wapp} and R_{gapp} against time t for T-jumps from ΔT_0 to ΔT with $\Delta T_0 < \Delta T$. With the lapse of time, M_{wapp} increases monotonically, whereas R_{gapp} first decreases and then increases to reach a new equilibrium value, showing a shallow minimum. As the polymer concentration decreases and ΔT_0 becomes smaller at the fixed ΔT, the changes are enhanced. The large increase of M_{wapp} with slight change of R_{gapp} implies that the increase of micellar fraction dominates over the growth in micellar size. Remembering that, at the beginning of the micellar relaxation, there remains an appreciable amount of unimers, one can easily conclude from the above observations that a large fraction of existing unimers form new micelles. Some part of unimers enter into existing micelles formed in the premicellization, because M_{wapp} and R_{gapp} were larger than those of micelles formed by a direct temperature jump from the unimer state, 60 °C, to those temperatures. The association number of newly created micelles must be a little smaller than that of previously formed micelles. This leads to the shallow minimum in the R_{gapp} vs t plot. The lower the polymer concentration is, or the shallower the depth ΔT_0 of premicellization is, the larger the amount of unimers that remains at the beginning (Figure 2), which results in the larger increment of M_{wapp} and the deeper minimum of R_{gapp}.

Relaxation of Micellization in Type II T-Jumps (Deep-to-Shallow Jumps). In Figures 5 and 6 are

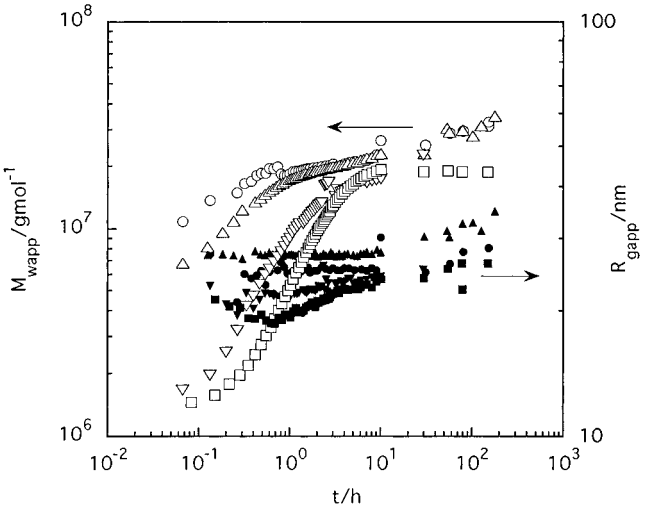

Figure 3. Time evolution of M_{wapp} and R_{gapp} for KT-327 solutions of various concentrations at 35 °C after premicellization at 45 °C. M_{wapp}: 8.146×10^{-4} g(g of solution)$^{-1}$ (○), 4.231×10^{-4} g(g of solution)$^{-1}$ (△), 2.378×10^{-4} g(g of solution)$^{-1}$ (▽), 1.693×10^{-4} g(g of solution)$^{-1}$ (□). R_{gapp}: 8.146×10^{-4} g(g of solution)$^{-1}$ (●), 4.231×10^{-4} g(g of solution)$^{-1}$ (▲), 2.378×10^{-4} g(g of solution)$^{-1}$ (▼), 1.693×10^{-4} g(g of solution)$^{-1}$ (■).

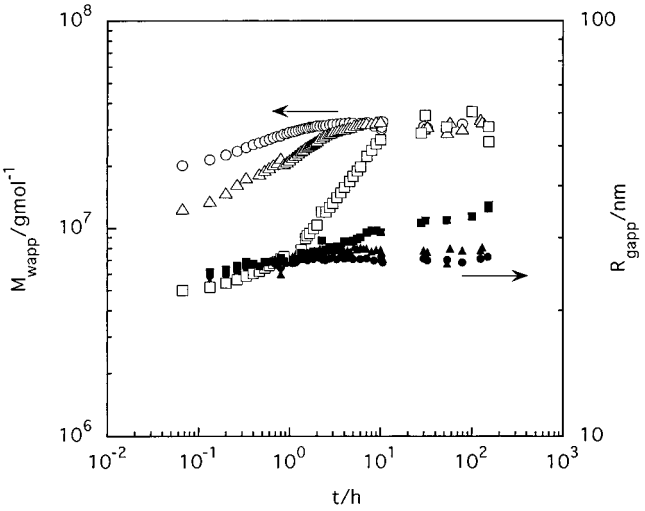

Figure 4. Time evolution of M_{wapp} and R_{gapp} KT-327 solutions of various concentrations at 35 °C after premicellization at 40 °C. M_{wapp}: 8.146×10^{-4} g(g of solution)$^{-1}$ (○), 4.231×10^{-4} g(g of solution)$^{-1}$ (△), 1.693×10^{-4} g(g of solution)$^{-1}$ (□). R_{gapp}: 8.146×10^{-4} g(g of solution)$^{-1}$ (●), 4.231×10^{-4} g(g of solution)$^{-1}$ (▲), 1.693×10^{-4} g(g of solution)$^{-1}$ (■).

shown log−log plots of M_{wapp} and R_{gapp} against time t for T-jump from ΔT_0 to ΔT with $\Delta T_0 > \Delta T$. With the lapse of time, both of M_{wapp} and R_{gapp} first decrease sharply and then increase to reach new respective equilibrium values, showing minima. As the polymer concentration decreases and ΔT becomes smaller at the fixed ΔT_0, the changes are enhanced, and the depths of the minima increase. At the smaller ΔT, 45 °C, M_{wapp} and R_{gapp} decrease faster and positions of the minima are located at shorter times. These time evolutions of M_{wapp} and R_{gapp} obviously indicate the followings. Instead of monotonical changes in micellar fraction and size from the starting state to the final state, the micelles first decompose with changing micellar size and/or number, and then, the micellar size and/or number recover to approach those at the final state. As the concentration becomes closer to the cmc, the observed changes become larger, in other words, the relaxation strengths become larger. The relaxation

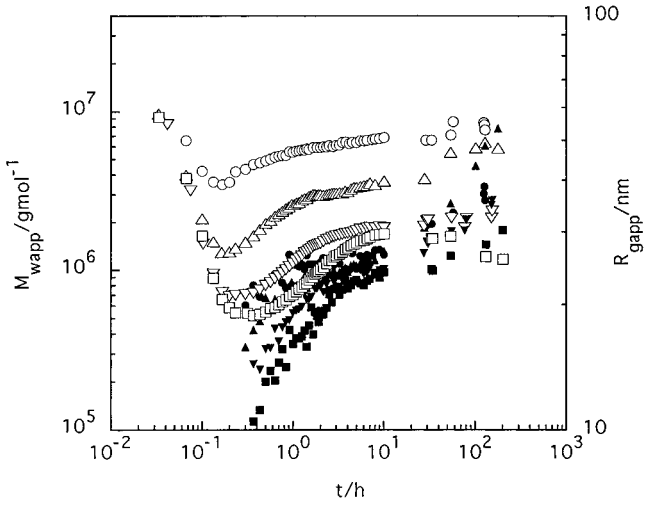

Figure 5. Time evolution of M_{wapp} and R_{gapp} for KT-327 solutions of various concentrations at 45 °C after premicellization at 35 °C. M_{wapp}: 8.146×10^{-4} g(g of solution)$^{-1}$ (○), 4.231×10^{-4} g(g of solution)$^{-1}$ (△), 2.378×10^{-4} g(g of solution)$^{-1}$ (▽), 1.693×10^{-4} g(g of solution)$^{-1}$ (□). R_{gapp}: 8.146×10^{-4} g(g of solution)$^{-1}$ (●), 4.231×10^{-4} g(g of solution)$^{-1}$ (▲), 2.378×10^{-4} g(g of solution)$^{-1}$ (▼), 1.693×10^{-4} g(g of solution)$^{-1}$ (■).

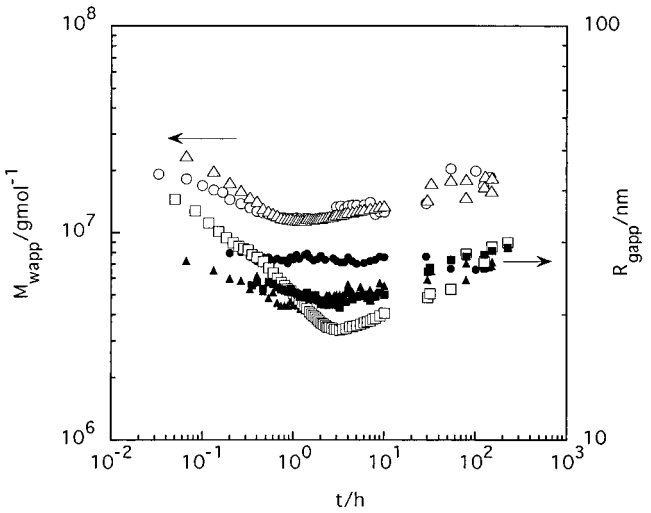

Figure 6. Time evolution of M_{wapp} and R_{gapp} for KT-327 solutions of various concentrations at 40 °C after micellization at and heating from 35 °C. M_{wapp}: 8.146×10^{-4} g(g of solution)$^{-1}$ (○), 4.231×10^{-4} g(g of solution)$^{-1}$ (△), 1.693×10^{-4} g(g of solution)$^{-1}$ (□). R_{gapp}: 8.146×10^{-4} g(g of solution)$^{-1}$ (●), 4.231×10^{-4} g(g of solution)$^{-1}$ (▲), 1.693×10^{-4} g(g of solution)$^{-1}$ (■).

process can be divided into two processes for convenience. In the decomposition process associated with decreasing M_{wapp} and R_{gapp}, it should be noted that M_{wapp} and R_{gapp} decrease in parallel. The parallel change implies that the decrease of the micellar size dominates over direct decomposition of micelles to unimers with decrease of micellar number. On the other hand, in the recovery process associated with the increase in M_{wapp} and R_{gapp} to the equilibrium state, the increase in M_{wapp} is a little gentler as compared with the increase of R_{gapp}. This is essentially a consequence of the requirement that the micellar fraction at the final state should be lower than at the initial state, and in other words, the micellar number must become lower at the end of the process because micellar size recovers to be comparative to, or rather larger than, the initial size at the late stage. Hence, this dominant increase of R_{gapp} over M_{wapp} suggests the growth and recovery of micellar size with decreasing number of micelles in the process of recovery. This suggestion is visualized in the time evolutions of M_{wapp} and R_{gapp} at the very late stage of relaxation, in particular an overshoot of M_{wapp} in the most dilute solution at the smaller ΔT. Namely, at the late stage at 45 °C (Figure 5), one finds a weaker increase of M_{wapp} at lower concentrations and even the decrease, i.e., the overshoot, in the most dilute solution, while R_{gapp} steadily increases with the lapse of time irrespective of the concentration. This finding clearly implies that the micellar number should appreciably be decreasing at the late stage, although the data at the late stage are somewhat fluctuating and scattered.

To summarize the present findings, the relaxation processes are here tentatively separated into four elemental characteristic processes, although sometimes these are not so clearly distinguished: (1) *growth* of micellar size with successive entry of unimers into micelles; (2) *diminishing* of micellar size with successive expulsion of unimers from micelles; (3) *birth* of new micelles, which is difficult to be distinguished from their growth in some cases; and (4) *extinction* or breaking of micelles into unimers, which difficult to distinguish from their diminishing in some cases. In terms of these processes, the relaxation kinetics can be summarized as follows: In the type I, shallow-to-deep T-jump, the relaxation proceeds by birth and growth of existing excess unimers and growth of micelles formed in the premicellization. In the type II, deep-to-shallow T-jump, the relaxation proceeds by decomposition with diminishing, followed by recovery with growth and, later, by simultaneous occurrence of growth and extinction with decrease of micellar number.

The processes in type I T-jumps can be understood, because the situation is similar to the micellization from the unimer state to the micellar state. However, processes in type II T-jumps are not so simple because the micellar solution does not change directly to the final state, but the micelles decompose first and then appear and grow again. A question that has arisen is why the micelles should decompose once. An answer has already been given, for instance, by the Aniansson−Wall theory for aqueous solution of low molecular weight surfactants. The answer for the present case must essentially be the same. Detailed discussion will come later.

Time Constants of Relaxation Processes. In the previous study of the direct micellization from the unimer state,[28] in order to evaluate representative time constants for the first and second processes, the growth of M_{wapp} was approximated by an exponential function with a single relaxation time for each process. That is,

$$M_{wapp} = M_u + (M_m - M_u)[1 - m_1\, exp(-t/\tau_1) - (1 - m_1)\exp(-t/\tau_2)] \quad (3)$$

with $\tau_1 < \tau_2$. Constants M_u and M_m correspond to molecular weights of a unimer and an equilibrium micelle, respectively, and m_1 is the fractional amplitude of the first process. In T-jumps of type I of the present study, the change of M_{wapp} exhibits a monotonical increase with time and could be approximated by a single exponential decay function:

$$M_{wapp} = M_u + (M_m - M_u)[1 - \exp(-t/\tau_I)] \quad (4)$$

On the other hand, for type II, at least two time constants are obviously needed to describe the results with decomposition and recovery processes. The present results could be approximated by a function of two

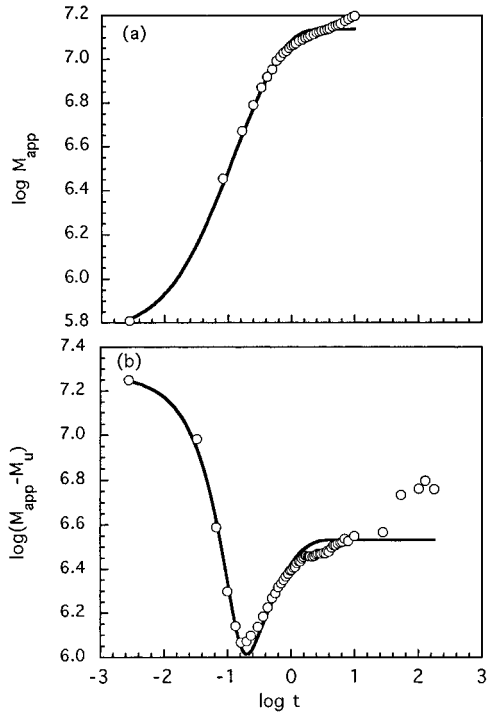

Figure 7. Examples of fitting curves for micellization: (a) $C = 4.231 \times 10^{-4}$ g(g of solution)$^{-1}$, $T = 35$ °C; (b) $C = 4.231 \times 10^{-4}$ g(g of solution)$^{-1}$, $T = 45$ °C.

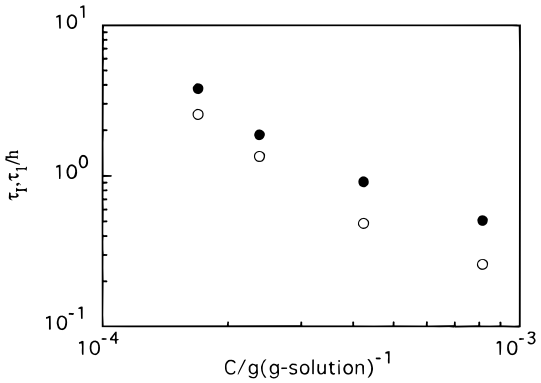

Figure 8. log−log plots of τ_I vs c for type I T-jumps: (●) type I T-jumps from 45 to 35 °C and (○) τ_1 for direct T-jumps from 60 to 35 °C.

single-exponential decays similar to eq 3:

$$M_{wapp} = M_u + (M_{m0} - M_u)\exp(-t/\tau_D) + (M_{m1} - M_u)[1 - \exp(-t/\tau_R)] \quad (5)$$

The amplitudes, $M_{m0} - M_u$ and $M_{m1} - M_u$ are those for the two processes. Time constants τ_D and τ_R along with the parameters $M_{m0} - M_{mu}$ and $M_{m1} - M_{mu}$ were obtained by the nonlinear least-squares fitting to eqs 4 and 5. Examples of fitting curves with the data are shown in Figure 7a,b. In most cases, M_{wapp} changes more gradually than the calculated curves by the single-exponential description, and the data at the very late stage deviate from the curve. However, the fittings were reasonably good enough to evaluate representative time constants for the relaxation processes of micellization. For comparison, the time constants for processes of direct micellization from the unimer state were also evaluated from the data of time evolution of M_{wapp}.

Type I T-Jumps. Figure 8 shows the time constant τ_I for type I T-jumps from 45 to 35 °C, along with those for direct micellization from the unimer state (60 °C →

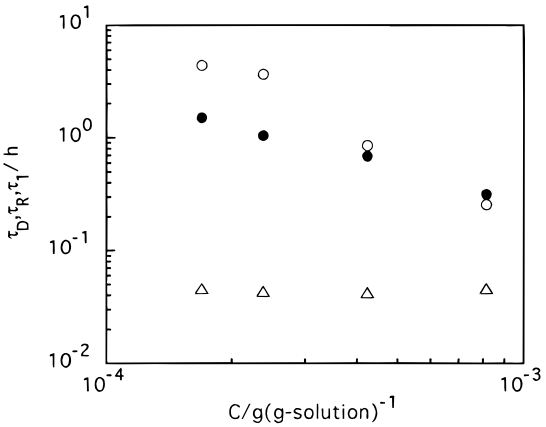

Figure 9. log−log plots of τ_D and τ_R vs c for type II T-jumps. τ_D (△) and τ_R (●) for type II T-jumps from 35 to 45 °C and τ_1 (○) for direct T-jumps from 60 to 45 °C.

35 °C). The time constant τ_I decreases with increasing polymer concentration. At lower concentrations, the τ_I is almost the same as the time constant τ_1 in the direct micellization. This is quite reasonable, since the unimer fraction in the total copolymer at the beginning is high at lower concentrations (see Figure 2), so the situation is similar to that in the direct micellization. On the other hand, at higher concentrations, the process is faster, which may come from that the higher concentration solutions have more existing micelles and fewer unimers, and the unimers may participate both in forming new micelles and entering into existing micelles.

Type II T-Jumps. Figure 9 represents the concentration dependencies of the time constant for decomposition (τ_D) and for recovery (τ_R), with the τ_1 of the direct micellization (60 °C → 45 °C) as a reference. The τ_D is independent of the concentration and much smaller than the τ_R. τ_R decreases with increasing concentration and is fairly close to the τ_1 of the direct micellization, especially at higher concentration. Namely, the recovery process proceeds at almost the same rate as the rate of direct micellization from unimer state, but not at exactly the same rate in low concentrations. This may imply that, although the amount of unimers produced in the decomposition process is large enough to realize a similar situation to the direct micellization, the situation is not the same as in the direct micellization. In type II T-jumps, there may remain small micelles produced in the first diminishing process which makes the recovering process faster, especially at lower concentrations.

Thermodynamical Interpretation. Relaxation kinetics of the present systems may essentially be explained by the A−W theory. Here, a thermodynamical interpretation will be presented to try to see the physics of the relaxation kinetics, confirm that the relaxation process in type II T-jumps is thermodynamically possible, and explain why the micelles are decomposed first. The interpretation is based on the following ideas. Free-energy balance between unimers and micelles controls the driving force and accordingly the rate of relaxation process, where chemical potential of the unimers does depend on the unimer concentration only. There exist two internal variables describing the state of the system, which have different rate constants: These are, for example, the number of micelles (M) and the association number (P), and entry (or expulsion) of unimers into (or out of) micelles occurs more easily than birth (or breaking) of micelles from (or to) unimers does even

under the same driving force.

A micellar solution is, for simplicity, approximated by a ternary mixture of unimers, micelles, and solvent with monodisperse distribution of the association number. We start with the following phenomenological kinetic equations for the association number (P) and the number of micelles (M) according to the thermodynamics for irreversible processes.[32] Namely, ignoring the *direct* cross-effects between P and M, one may have

$$\frac{\mathrm{d}P}{\mathrm{d}t} = -L_P\left(\frac{\partial F}{\partial P}\right)_M \tag{6}$$

$$\frac{\mathrm{d}M}{\mathrm{d}t} = -L_M\left(\frac{\partial F}{\partial M}\right)_P \tag{7}$$

where F is the free energy of the system, and L_P and L_M correspond to phenomenological Onsager coefficients for the rates of P and M, respectively. Volume fractions of unimers, micelles, and solvent, which are denoted as ϕ_u, ϕ_m, and ϕ_s, respectively, can be written as

$$\phi_\mathrm{u} = (N - PM)(v_\mathrm{u}/V) \qquad \phi_\mathrm{m} = PM(v_\mathrm{u}/V)$$
$$\phi_\mathrm{s} = 1 - \phi_\mathrm{u} - \phi_\mathrm{m} \tag{8}$$

with N being the total number of polymer molecules and v_u and V the volumes of unimer and solution, respectively. Assuming that the solution is dilute enough, the free energy (F) can be given by the sum of free energies of respective components as

$$F = V(kT/v_\mathrm{u})[\phi_\mathrm{m} f_\mathrm{m}(P,\phi_\mathrm{m}) + \phi_\mathrm{u} f_\mathrm{u}(\phi_\mathrm{u}) + \phi_\mathrm{s} f_\mathrm{s}(\phi_\mathrm{s})] \tag{9}$$

where the free energy $f_\mathrm{m}(P,\phi_\mathrm{m})$ of micelles is a function of P and ϕ_m, and those of unimer and solvent, $f_\mathrm{u}(\phi_\mathrm{u})$ and $f_\mathrm{s}(\phi_\mathrm{s})$, are functions of respective volume fractions. Here, the free energy densities (f) are per unimer volume. $f_\mathrm{m}(P)$ and $f_\mathrm{u}(\phi_\mathrm{u})$ can be expressed as

$$f_\mathrm{m}(P,\phi_\mathrm{m}) = \frac{1}{P}\ln\phi_\mathrm{m} + a_\mathrm{m}(P) \tag{10}$$

$$f_\mathrm{u}(\phi_\mathrm{u}) = \ln\phi_\mathrm{u} + a_\mathrm{m}(1) \tag{11}$$

with the free energy density $a_\mathrm{m}(P)$ of a micelle given as a function of P only. Then, one has

$$\left(\frac{\partial F}{\partial P}\right)_M/M = kT\left[\frac{\mathrm{d}(a_\mathrm{m}P)}{\mathrm{d}P} + \phi_\mathrm{m} - \ln\phi_\mathrm{u} - a_0\right] = kT(A_P - A_\mathrm{u}) \tag{12}$$

$$\left(\frac{\partial F}{\partial M}\right)_P/P = kT\left(a_\mathrm{m} + \frac{1}{P}\ln\phi_\mathrm{m} - \ln\phi_\mathrm{u} - a_0\right) = kT(A_M - A_\mathrm{u}) \tag{13}$$

where $a_0 = a_\mathrm{m}(1) + 1$ and the affinities (A) are

$$A_P = \mathrm{d}(a_\mathrm{m}P)/\mathrm{d}P + \phi_\mathrm{m} - a_0 = a_\mathrm{m} + Pa'_\mathrm{m} + \phi_\mathrm{m} - a_0 \tag{14}$$

$$A_M = a_\mathrm{m} + \frac{1}{P}\ln\phi_\mathrm{m} - a_0 \tag{15}$$

$$A_\mathrm{u} = \ln\phi_\mathrm{u} \tag{16}$$

The prime denotes the differential with respect to P, i.e., $a'_\mathrm{m} = \mathrm{d}a_\mathrm{m}/\mathrm{d}P$. Then, the kinetic equations of eqs 6 and 7 are expressed as

$$\frac{\mathrm{d}P}{\mathrm{d}t} = -\bar{L}_P(A_P - A_\mathrm{u})(Mv_\mathrm{u}/V) \tag{17}$$

$$\frac{\mathrm{d}(Mv_\mathrm{u}/V)}{\mathrm{d}t} = -\bar{L}_M(A_M - A_\mathrm{u})P \tag{18}$$

Here, we put the coefficients $\bar{L}_P = (kTV/v_\mathrm{u})L_P$ and $\bar{L}_M = (kTv_\mathrm{u}/V)L_M$ so as to be intensive quantities. At equilibrium, since

$$\left(\frac{\partial F}{\partial P}\right)_M = \left(\frac{\partial F}{\partial M}\right)_P = 0 \tag{19}$$

one has

$$A_P = A_M = A_\mathrm{u} \tag{20}$$

and these affinities are equivalent to the chemical potential in unit of kT/v_u. From eq 20 with eqs 14−16, the following relations are deduced for quantities with subscript e denoting the equilibrium state.

$$a_\mathrm{me} - a_0 = \ln\phi_\mathrm{ue} - \frac{1}{P_\mathrm{e}}\ln\phi_\mathrm{me} \tag{21}$$

$$P_\mathrm{e}a'_\mathrm{me} = \frac{1}{P_\mathrm{e}}\ln\phi_\mathrm{me} - \phi_\mathrm{me} \tag{22}$$

To have explicit formulae for $A_P - A_\mathrm{u}$ and $A_M - A_\mathrm{u}$, we may express the functions of $(a_\mathrm{m} - a_0)$ and a'_m as

$$a_\mathrm{m} - a_0 = g(\Delta P) + a'_\mathrm{me}\Delta P + a_\mathrm{me} - a_0 \tag{23}$$

$$a'_\mathrm{m} = g'(\Delta P) + a'_\mathrm{me} \tag{24}$$

with $\Delta P \equiv P - P_\mathrm{e}$ and the function $g(\Delta P)$ defined here must disappear at equilibrium, $\Delta P = 0$. A most simple formula for $g(\Delta P)$ may be

$$g(\Delta P) = k(\Delta P)^2 \tag{25}$$

with k being a constant which is positive because of the stability of micelles at $\Delta P = 0$. Equations 14−16 can be transformed by eqs 21−24 to be

$$A_M - A_\mathrm{u} = g(\Delta P) + \left(\frac{\ln\phi_\mathrm{m}}{P} - \frac{\ln\phi_\mathrm{me}}{P_\mathrm{e}}\right) + \ln(\phi_\mathrm{ue}/\phi_\mathrm{u}) \tag{26}$$

$$A_P - A_\mathrm{u} = g(\Delta P) + Pg'(\Delta P) + \frac{2\Delta P}{P_\mathrm{e}}\left(\frac{1}{P_\mathrm{e}}\ln\phi_\mathrm{me} - \phi_\mathrm{me}\right) + (\phi_\mathrm{m} - \phi_\mathrm{me}) + \ln(\phi_\mathrm{ue}/\phi_\mathrm{u}) \tag{27}$$

with eq 25. Now, for a given set of ϕ_ue and P_e with their initial values of ϕ_u0 and P_0, we can calculate time evolutions of P and Mv_u/V as a function of the total polymer concentration $\phi_\mathrm{m} + \phi_\mathrm{u}$ ($=\phi_\mathrm{me} + \phi_\mathrm{ue}$), if the constant k is given, by solving the simultaneous eqs 17 and 18 with eqs 25−27. Note here that ϕ_ue is the critical micelle concentration when $\phi_\mathrm{m} + \phi_\mathrm{u} \gg \phi_\mathrm{ue}$. If time evolutions of P and M are obtained, we can calculate ϕ_m or ϕ_u, A_u, A_M, A_P, and the free energy F as functions of time, and time evolutions of M_wapp and R_gapp as well, if R_g can be evaluated as a function of P. That is,

$$M_\mathrm{wapp}/M_\mathrm{u} = [MP^2 + (N - MP)]/N \tag{28}$$

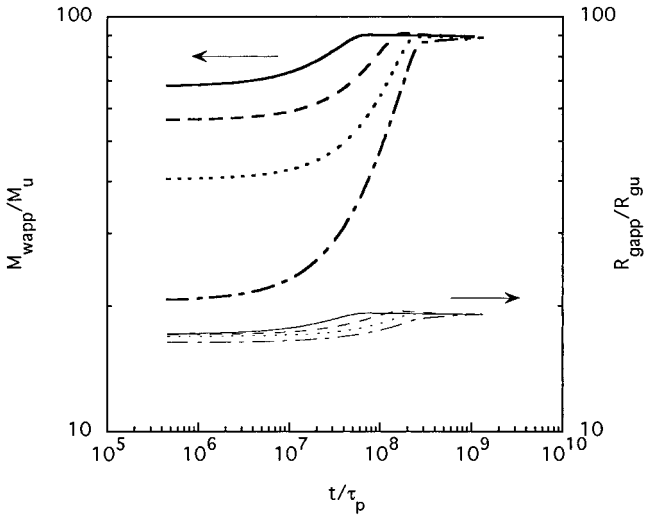

Figure 10. Time evolution of M_{wapp} and R_{gapp} for type I T-jumps, calculated on the basis of eqs 17 and 18. $P_0 = 80$, $P_e = 90$, $\phi_{u0} = 6 \times 10^{-7}$, $\phi_{ue} = 1 \times 10^{-8}$, $k = 2 \times 10^{-3}$, $\tau_P = 1 \times 10^{-6}$, $\tau_P/\tau_M = 1 \times 10^{-19}$; polymer concentration $\phi_m + \phi_u$ ($=\phi_{me} + \phi_{ue}$) $= 1.2 \times 10^{-6}$ (– - –), 2×10^{-6} (- -), 4×10^{-6} (– –), and 8×10^{-6} (—). M_{wapp}, thick lines; R_{gapp}, thin lines.

$$R_{gapp}/R_{gu} = [MP^2P^{\nu} + (N - MP)]/[MP^2 + (N - MP)] \quad (29)$$

where R_g of a micelle with molar mass of M_w is given by $R_g = R_{gu}P^{\nu}$ with $\nu = 0.3$[27,31]

Calculated results for T-jumps of types I and II are presented in Figures 10 and 11, respectively. The time scale was given in terms of the time constant defined as

$$\tau_P = 1/\bar{L}_P$$

$$\tau_M = 1/\bar{L}_M$$

The parameters used are indicated in the figure captions. The phenomenological time constants were provided appropriately such that the calculated M_{wapp} and R_{gapp} reproduce the experimental ones as well as possible.

The type I T-jump is characterized by the condition that the initial unimer concentration is higher than the critical micelle concentration, $\phi_{u0} > \phi_{ue}$. In Figure 10 are shown the calculated results for this condition as a function of polymer concentration with the other parameters being fixed. The results for M_{wapp} and R_{gapp} can reproduce the observations for concentration and quench depth dependencies of the time evolution of M_{wapp}. The increase of M_{wapp} is brought about dominantly by birth of new micelles with decreasing the unimer concentration. This process is drived by the gap of affinities between A_M and A_u with $A_M < A_u$ because the unimer concentration is high enough, $\phi_{u0} > \phi_{ue}$. The observed small dip of the R_{gapp}–time curve at lower concentration cannot be explained by the model probably because of the assumption of monodisperse distribution of micellar size.

Figure 11a shows the calculated results of M_{wapp} and R_{gapp} for the type II T-jump, where $\phi_{u0} < \phi_{ue}$. The calculated curves well-reproduce the sharp decrease and recovery of M_{wapp} and R_{gapp} and the enhancement of these changes with decreasing concentration. In parts b and c of Figure 11 are shown time evolutions of P, M, ϕ_u, A_P, A_M, A_u, and F for the lowest concentration in part a. At the beginning of the relaxation, the positive

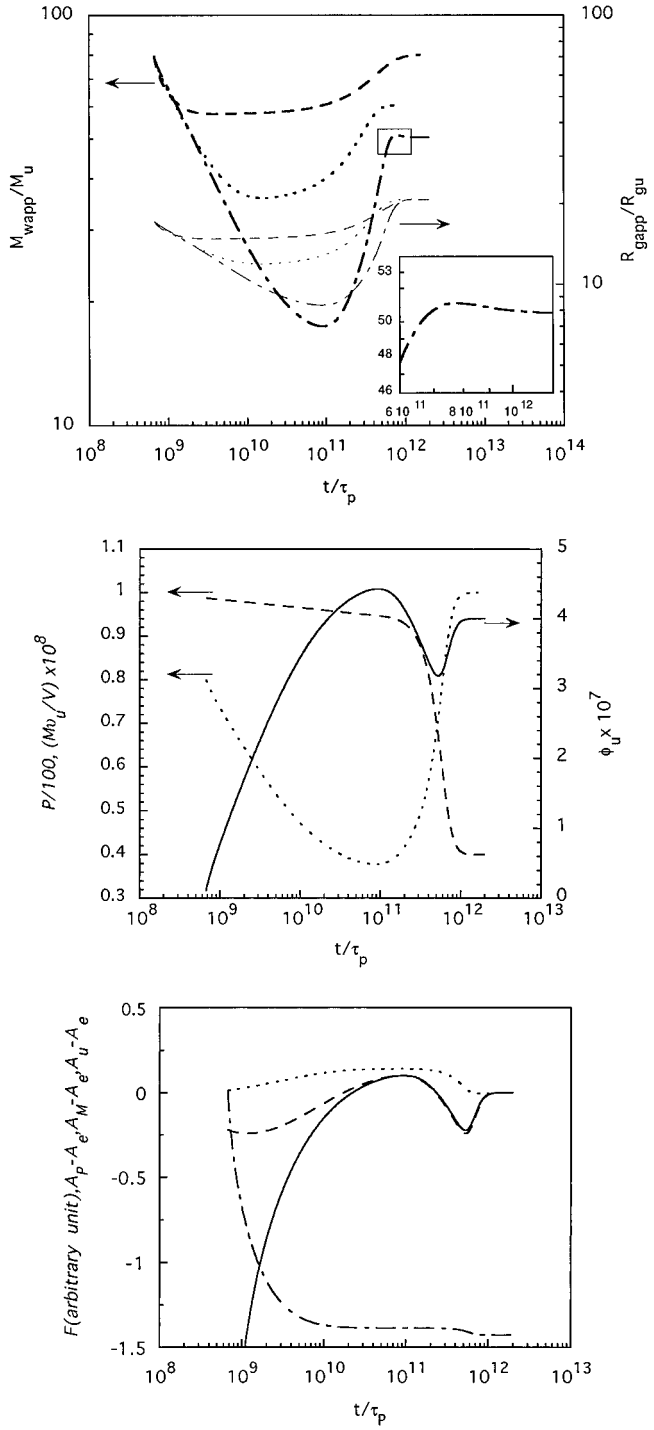

Figure 11. Time evolutions of M_{wapp} and R_{gapp} and other quantities for type II T-jumps, calculated on the basis of eqs 17 and 18. $P_0 = 80$, $P_e = 100$, $\phi_{u0} = 1 \times 10^{-6}$, $\phi_{ue} = 4 \times 10^{-7}$, $k = 1 \times 10^{-4}$, $\tau_P = (1/1.5) \times 10^{-9}$, $\tau_P/\tau_M = (1/1.5) \times 10^{-21}$. (a) M_{wapp} and R_{gapp} polymer concentration [$\phi_m + \phi_u$ ($=\phi_{me} + \phi_{ue}$)]: 0.8×10^{-6} (– - –), 1×10^{-6} (- -), and 2×10^{-6} (– –). M_{wapp}, thick lines; R_{gapp}, thin lines. The inset shows a partially enlarged curve for $\phi_m + \phi_u = 0.8 \times 10^{-6}$. (b) P (- -), $M\upsilon_u/V$ (– –), and ϕ_u (—); polymer concentration 0.8×10^{-6}. (c) Affinities $A_P - A_e$ (– –), $A_M - A_e$ (- -), and $A_u - A_e$ (—) and the free energy F (– - –); A_e is the value at the final state for A_P, A_M, and A_u (see eq 20); polymer concentration 0.8×10^{-6}.

gap of $A_P - A_u$, which is a result of ϕ_{u0} being lower than ϕ_{ue}, drives and promotes the decrease of association number (P), which brings about the decreases of both M_{wapp} and R_{gapp}. As this diminishing process proceeds, the unimer concentration increases, the A_u increases rapidly to exceed the affinity A_p, and the sign of the gap

$A_P - A_u$ becomes negative. The change of sign brings about the increase of P, recovering M_{wapp} and R_{gapp}. The change of sign possibly takes place because of the slow change of M, which prevents the system from directly reaching the final state by one step. During the time evolution of P and M, the free energy of the system always keeps decreasing with lapse of time as is thermodynamically required. In the late stage, M decreases, accompanying the increase of P, and leads to the increase of ϕ_u with time under a certain condition of balances between L_P and L_M and/or among A_P, A_M, and A_u. The decrease of M with increasing ϕ_u, which dominates over the increase of P, is responsible for the decrease of M_{wapp}, i.e. the overshoot at the final stage. (See the inset of Figure 11a.) This is exactly consistent with the observation. The calculated results of time evolutions of M_{wapp}, R_{gapp}, P, and M qualitatively reproduce well the present observations and are consistent with the interpretations in the previous section. The observed changes of micellar solution in the type II T-jump have been demonstrated to be thermodynamically possible. However, quantitative agreements between experiments and calculations are not so good, in particular, for the magnitude of large decrease of M_{wapp} and R_{gapp} in type II T-jumps at lower concentrations. This is because the theory is essentially a linear one which cannot be applied to a large quench depth except near the equilibrium.

References and Notes

(1) Muller, N. *J. Phys. Chem.* **1972**, *21*, 3017.
(2) Tuzar, Z.; Petrus, V.; Kratochvil, P. *Makromol. Chem.* **1974**, *175*, 3181.
(3) Aniansson, E. A. G.; Wall, S. N. *J. Phys. Chem.* **1974**, *78*, 1024.
(4) Nakagawa, T. *Colloid Polym. Sci.* **1974**, *252*, 56.
(5) Aniansson, E. A. G.; Wall, S. N. *J. Phys. Chem.* **1975**, *79*, 857.
(6) Lang, J.; Tondre, C.; Zana, R.; Bauer, R.; Hoffmann, H.; Ulbricht, W. *J. Phys. Chem.* **1975**, *79*, 276.
(7) Aniansson, E. A. G.; Wall, S. N.; Almgren, M.; Hoffmann, H.; Kielmann, I.; Ulbricht, W.; Zana, R.; Lang, J.; Tondre, C. *J. Phys. Chem.* **1976**, *80*, 905.
(8) Hoffmann, H.; Nagel, R.; Platz, G.; Ulbricht, W. *Colloid Polym. Sci.* **1976**, *254*, 812.
(9) Hoffmann, H.; Kielmann, I.; Pavlovic, D.; Platz, G.; Ulbricht, W. *J. Colloid Interface Sci.* **1981**, *80*, 237.
(10) Kahlweit, M.; Teubner, M. *Adv. Colloid Interface Sci.* **1980**, *13*, 1.
(11) Lessner, E.; Teubner, M.; Kahlwelt, M. *J. Phys. Chem.* **1981**, *85*, 1529.
(12) Lessner, E.; Teubner, M.; Kahlwelt, M. *J. Phys. Chem.* **1981**, *85*, 3167.
(13) Aniansson, E. A. G. In *Aggregation Processes in Solution*; Wyn-Jones, E., Gormally, J., Ed.; Elsevier: Amsterdam, 1983; Vol. 26, p 70.
(14) Kahlweit, M. In *Physics of Amphiphiles: Micelles Vesicles and Microemulsions*; Degiorgio, V., Corti, M., Ed.; North-Holland: Amsterdam, 1985; p 212.
(15) Lang, L.; Zana, R. In *Surfactant Solutions, Surfactant Science Series*; Zana, R., Ed.; Marcel Dekker: New York, 1986; Vol. 22, p 405.
(16) Bednar, B.; Edwards, K.; Almgren, M.; Tormod, S.; Tuzar, Z. *Makromol. Chem., Rapid Commun.* **1988**, *9*, 785.
(17) Hecht, E.; Hoffmann, H. *Colloids Surf., A* **1995**, *96*, 181.
(18) Halperin, A.; Alexander, S. *Europhys. Lett.* **1988**, *6*, 329.
(19) Halperin, A.; Alexander, S. *Macromolecules* **1989**, *22*, 2403.
(20) Halperin, A.; Tirrell, M.; Lodge, T. P. *Adv. Polym. Sci.* **1992**, *100*, 31.
(21) Wang, Y.; Mattice, W. L. *Langmuir* **1993**, *9*, 66.
(22) Wang, Y.; Kausch, C. M.; Cun, M.; Quirk, R. P.; Mattice, W. L. *Macromolecules* **1995**, *28*, 904.
(23) Wang, Y.; Mattice, W. L.; Napper, D. *Macromolecules* **1992**, *25*, 4073.
(24) Zhan, Y.; Mattice, W. L. *Macromolecules* **1994**, *27*, 677, 683.
(25) Wang, Y.; Balaji, R.; Quirk, R. P.; Mattice, W. L. *Polym. Bull.* **1992**, *28*, 333.
(26) Haliloglu, T.; Mattice, M. L. *Chem. Eng. Sci.* **1994**, *17*, 2851.
(27) Honda, C.; Hasegawa, Y.; Hirunuma, R.; Nose, T. *Macromolecules* **1994**, *27*, 7660.
(28) Yuan, X.-F.; Masters, A. J.; Price, C. *Macromolecules* **1992**, *25*, 6876.
(29) Quintana, J. R.; Villacampa, M.; Katime, I. A. *Macromolecules* **1993**, *26*, 601.
(30) Hirao, A.; Yamamoto, A.; Takenaka, K.; Yamaguchi, K.; Nakahama, S. *Polymer* **1987**, *28*, 303.
(31) Honda, C.; Sakaki, K.; Nose, T. *Polymer* **1994**, *35*, 5309.
(32) Prigogine, I. *Introduction to Thermodynamics of Irreversible Processes*, 3rd ed.; John Wiley & Sons, 1967; Chapter V, p 55. Meixner, J.; *Kolloid-Z.* **1953**, *134*, 3.

MA960735H